RESEARCHES REGARDING THE MICROANALYSIS RESULTS OPTIMISATION ON MULTILAYER NANOSTRUCTURES INVESTIGATIONS

F. MICULESCU[*], I. JEPU[a], C.P. LUNGU[a], M. MICULESCU, M. BANE
Politehnica University of Bucharest, Faculty of Materials Science and Engineering, Bucharest, 060042, Romania
[a]*National Institute for Laser, Plasma and Radiation Physics, Bucharest-Magurele, 077125, Romania*

In this paper we analyzed the chemical composition of a multilayered nanostructure using a perpendicularly incidence of accelerated electron beam at variable voltage, in order to have an X-ray signal that originates mainly from the desired layer to be investigated. In order to improve the results quality, we proposed a multilayer coating of a thicker layer from chemical elements that do not exist in the analyzed structure, elements having very different atomic number and no emission line that may overlap with the ones of elements of interest. The multilayer was Cu-Ni-Cu-Fe-Ta type nanostructure and we used a supplementary silver coating layer. This analysis can lead to the fact that, depending on the analyzed chemical elements and their layers thickness, additional coatings can be used (having thickness of a few hundreds of nanometers), of various chemical elements, to study quite precisely the proportion of chemical elements deposited as nanolayers and the depth to which they are located.

1. Introduction

Due to the latest deposition methods development, currently it is possible to deposit thin layers of nanometric dimensions, from different materials, in countless combinations. With the increasing performance of deposition facilities, it became necessary to improve the resolution in terms of imaging and elements separation within the microanalytical methods. Data provided by recent bibliographic materials give along other methods of analysis, the high resolution scanning electron microscopy (HRSEM), high-resolution transmission electron microscopy (HRTEM), electron energy loss spectroscopy (EELS) and last but not least the energy dispersive spectroscopy (EDS). [1-3] The advantages of using these methods are undeniable, from the details of imaging performance and determining the exact composition of the nanostructures in any form point of view, but without doubt, involve high costs from buying high performance equipment and ending with maintenance and consumables price.

In these respect, in this paper, we propose the use of EDS method, usable along the usual tungsten filament emission SEM microscopes, which involves significant cost reductions for all items above but allow nanolayers identification. More specifically, we try to analyze the chemical composition of some multilayer nanostructures using a perpendicularly incidence of accelerated electron beam at variable voltage, in order to have an X-ray signal that originates mainly from the desired layer to be investigated.

The literature indicates several possibilities to use the EDS method in the analysis of multilayer structures, but gives no certainty of accuracy when investigating nanostructures, due to the large depth of penetration of the accelerated beam energy, so that characteristic X-ray signals to be obtained from the desired depth. [4-6]

---

[*] Corresponding author: f_miculescu@yahoo.com

In order to improve the results quality in these cases, the team proposes a multilayer coating with thicker layers from chemical elements that do not exist in the analyzed structure, elements having very different atomic number and no emission line that may slightly overlap with the elements of interest.

In terms of physical phenomena, when high energy electrons interact with the sample, elastic or inelastic scattering is produced. Elastic scattering produces backscattered electrons (BSE), which are actually scattered incident electrons by the atoms from the sample. Inelastic scattering produces secondary electrons (SE), which are ejected electrons from the atoms in the sample. Electron scattering leads to changes in the direction of penetration of electrons in the sample surface. The interaction of the accelerated electron beam and atoms from the sample is produced in a given volume below the surface. This area is commonly described as pear-shaped and its size increases with the increase of incidence electron energy within the sample surface. In addition to BSE and SE electrons in the interaction X-rays are produced and used in microanalysis. SE have the energy level of a few keV, and within the zone of interaction they can escape only from a volume close to the surface from a depth of about 5 to 50nm, even if they are generated throughout the interaction volume. In contrast, BSEs have an energy level close to that of incidence electrons, allowing them to escape from a much deeper level of interaction volume, about 50 - 300nm. The spatial resolution of SEM images is significantly affected by the volume size from which the electron signal comes. [1, 3, 7, 8]

X-ray spectroscopy methods determine the presence and quantity of chemical elements by detecting the characteristic X ray emitted from atoms irradiated with high energy beams. Characteristic X-ray energy is given by the difference in energy between two electrons located on different layers and is well defined and dependent on the atomic number of the atom. X-rays are separated in the series *K*, *L* and *M* in accordance with the layers that electrons are filling. The atom ability to generate characteristic X-ray photons varies when irradiated with photons or characteristic X-rays electrons. There is primarily an emission competition between the X-ray photons and Auger electrons when the electron refills a vacancy on an inner layer and a secondarily competition in generating *K*, *L* and *M* series of X rays. Another difference between *K*, *L* and *M* lines is their energy levels. *K* series energy is the biggest, followed by the *L* and *M* series. Generally, there is a bigger probability that *L* lines of heavy elements to be detected than *K* lines, since the latter have energies greater than 20keV. [9, 10, 11]

EDS spectra are representations of X-ray lines intensity depending on the energy that ranges between 0.1 and 20keV and may include both heavy and light elements, because the *K* lines of light elements and *M* and *L* of heavy elements are located in this area. Lateral size of the interaction volume may be significantly greater than the diameter of the electron beam, which is very important when EDS analysis is used on micro-areas of massive samples.

2. Experimental

X-ray emission volume is represented by the area in which the primary beam energy is still higher than the energy required for excitation of certain lines of X-ray (E_{ex}). The emission volume is determined by the electron acceleration voltage (E_0) and the characteristics of the sample chemical elements, such as mass density (ρ) and E_{ex}. Emission volume was estimated as the depth of characteristic X ray generation (R) and it is considered that the lateral size of the emission volume is approximately equal to its depth, so R represents the spatial resolution in EDS microanalysis.

$$R = \frac{0.064(E_0^{1.7} - E_{ex}^{1.7})}{\rho}$$ (1)

The resolution can be improved by reducing the electron beam acceleration voltage (E_0), for the characteristic lines of different elements being important that the acceleration voltage to be close to the energy required for elements characteristic X-ray excitation. The general expression

for quantitative analysis involving standard samples is expressed by an equation that includes the matrix effects. [1, 4]

$$\frac{c_i}{c_{(i)}} = (Z_i A_i F_i)\frac{I_i}{I_{(i)}} = (Z_i A_i F_i)k_i \qquad (2)$$

The expression ($Z_i A_i F_i$) represents the matrix factors affecting the X-ray intensity of the i element in the sample (I_i) and standard sample ($I_{(i)}$), which can be divided into three main types: the effect of atomic number (Z_i), the absorption of X ray (A_i) and X-ray fluorescence (F_i).

The atomic number (Z) factor quantifies the difference in X-ray generation due to the changes in atomic number in the matrix and due to backscattering phenomena (R) and electrons retardation (S). A part of the primary electrons ($R<1$) is backscattered and does not generate X-rays, the backscattering effect being a function of atomic number. A chemical element present in a matrix of heavier elements will generate a signal with a lower intensity than that which might occur in an analysis of the element in pure form. The electron retardation is the continued loss of electrons energy that occurs on the electron trajectory due to inelastic scattering and is expressed as a retardation factor (S). [3]

$$S = \frac{1}{\rho} \cdot \frac{dE_0}{ds}, \qquad (3)$$

S being a function of distance traveled by the electrons in the sample (s), the electron acceleration voltage (E_0) and sample density (ρ). S decreases while R increases with increasing atomic number. The absorption factor (A) quantifies the decrease of the characteristic X-ray density from the emission to the detector.

$$I_x = I_0 \cdot \exp\left[-(\mu/\rho) \cdot \rho \cdot t\right] \qquad (4)$$

The absorption is strongly affected by the absorption coefficient (μ), density (ρ) and trajectory length (t) of the X-rays through the sample before reaching the surface.

The fluorescence factor (F) comes from the analyzed element characteristic X-ray excitation by the matrix atoms emitted characteristic X-ray. This phenomenon occurs when the matrix elements characteristic X rays have higher energy than is necessary for the excitation of the analyzed element X-rays. Thus, the resulted X-ray intensities of the analyzed element are multiplied by the fluorescence effect. [1-4]

ZAF method is based on the assumption that the sample is massive and has a microscopically flat surface. This is important in the analysis of thin films, whereas the matrix effect is reduced. Standardless method is recommended when standard samples are not available and it is based on the X-ray intensity that should be obtained from a standard of a pure element, in the same instrumental conditions. This method is used mostly when the sample is composed of transition elements which have K lines between 5 and 10keV. For items that have the K lines at less than 3keV significant errors can occur due to detection of several families of K, L and M lines. [1, 3, 4]

The multilayer Cu-Ni-Cu-Fe-Ta type nanostructures used for analysis in this paper were obtained using TVA method (detailed described in other papers) at the National Institute of Laser, Plasma and Radiation Physics (INFLPR), Bucharest-Magurele. [12-13] In the experiments presented in this paper, the voltage applied to the anode, had values of kV order (Table 1). To achieve nanodimensional multilayer films, we used a special anode system, consisting from a cylindrical graphite disc, in which there were positioned four crucibles with the specific deposition materials (Cu, Ni, Fe, Ta), each material being deposited in the necessary order, without external interference during the deposition session. [11].

The substrate used consisted of Si wafers (100) 10x12 mm, positioned at a distance of 250mm from the discharger. The deposition rates of each material were determined during the deposition process with a quartz microbalance. The deposition conditions and the thin layers thicknesses are presented in Table 1.

Similar samples, with the same structures, were further used for depositing an additional layer of 500nm of silver, the total thickness of the layers becoming 515, 523, 543 and 703nm

respectively. After deposition, the samples were placed in the working chamber of the SEM microscope for analysis by standardless method. Resulted images were obtained with a Philips XL 30 ESEM TMP microscope and the generated X-ray spectra were determined and analyzed by an energy dispersive spectrometer EDAX Sapphire, with 128eV resolution, at University "Politehnica" from Bucharest. Depending on electron beam accelerating voltage and the analyzed elements *K*, *L* and *M* emission lines were used. [14, 15]

Table 1. Operating parameters and thickness of deposited layers.

Elem.	U (V)	I (mA)	Rate (Å/s)	1st Structure thickness (nm)	2nd Structure thickness (nm)	3rd Structure thickness (nm)	4th Structure thickness (nm)
Cu	600	350	6	3	5	10	50
Ni	1300	50	0.1	3	5	10	50
Cu	1800	90	0.2	3	5	10	50
Fe	2100	120	0.2	3	5	10	50
Ta	1500	110	0.1	3	3	3	3
Total				15	23	43	203

We studied the effect of electron beam energy (ranging between 5 and 30 kV in steps of 5 kV for 150 life seconds) on the penetration depth into the nanostructurated multilayers. The dead time during the spectrum collection was kept below 40%. Samples were positioned at a take off angle (TOA) of 35º from X-ray detector. During tests, the working conditions were kept in order to minimize any effect on the statistical nature of the production of radiation. Using the EDAX analysis software, the results were normalized using the ratio of the intensity spectrum. The magnitude of errors should not be significant in this study, as operating conditions were optimized. [11]

As layers were deposited from chemical elements having a close *Z* number the structures being similar, but with very different thicknesses, it is assumed that a proper analysis should highlight approximately double *Cu* concentrations compared to the cumulative signal of *Ni* and *Fe*. We will determine the recommended acceleration voltage for the nanodimensional multilayer structures analysis function of the analyzed layers thickness. Since the energies depth of penetration required to obtain characteristic X-ray are known to be of micrometer size for light elements and close to a micrometer for the heavy elements, it is possible that the initial assumption is not outlined in any of the studied cases. For this reason, in order to obtain at higher accelerating voltages, required for the excitation of *K* lines of heavy elements, results closer to the assumption that in terms of wt% concentrations *Cu=Ni+Fe*, we also performed EDS microanalysis on samples with structures similar to the first samples, over which a layer of 500nm of *Ag* was deposited. Silver was chosen because the difference in atomic number is large enough and there is no overlap for either of the spectral lines of interest.

3. Results and discussion

EDS analysis of the first Cu-Ni-Cu-Fe samples, without the silver supplementary layer deposited, resulted in six X-ray emission spectra for each set of samples, at 5, 10, 15, 20, 25 and 30 kV electron beam accelerating voltage, in perpendicular incidence to the electron beam at a TOA of 35° relative to the spectrometer X-ray detector. The results were used to plot the curves of variation of elemental concentrations (wt %) with the e-beam acceleration voltage.

The analysis of 3nm layers having a total thickness of 15nm, showed increasing *Ta* concentration (upper) from 54% at 5kV, to 67% at 15kV, and 70% at 30kV respectively. Using 20, 25 and 30kV accelerating voltage led to similar concentrations of *Ta*, which leads to the conclusion that the shape and size of the interaction volume of accelerated electrons with the nanodimensional multilayer have a reduced influence on the results obtained by analyzing the upper layers. The concentration of *Fe* layer interfaced with *Ta* layer and upper layer of *Cu* decreased from 6.5% to 0.6% at 15kV, and to 0.25% at 30kV respectively. Similarly with the

analysis of the *Ta* layer, the concentration of *Fe* varied slightly at accelerating voltage bigger than 15 kV, so the X-rays signal, at these voltages, comes from the depth of the interaction volume. The quantitative determinations of *Cu* showed significant variations function of accelerating voltage from 10% at 5kV, to 1.5% at 15kV, and 0.3% at 30kV respectively.
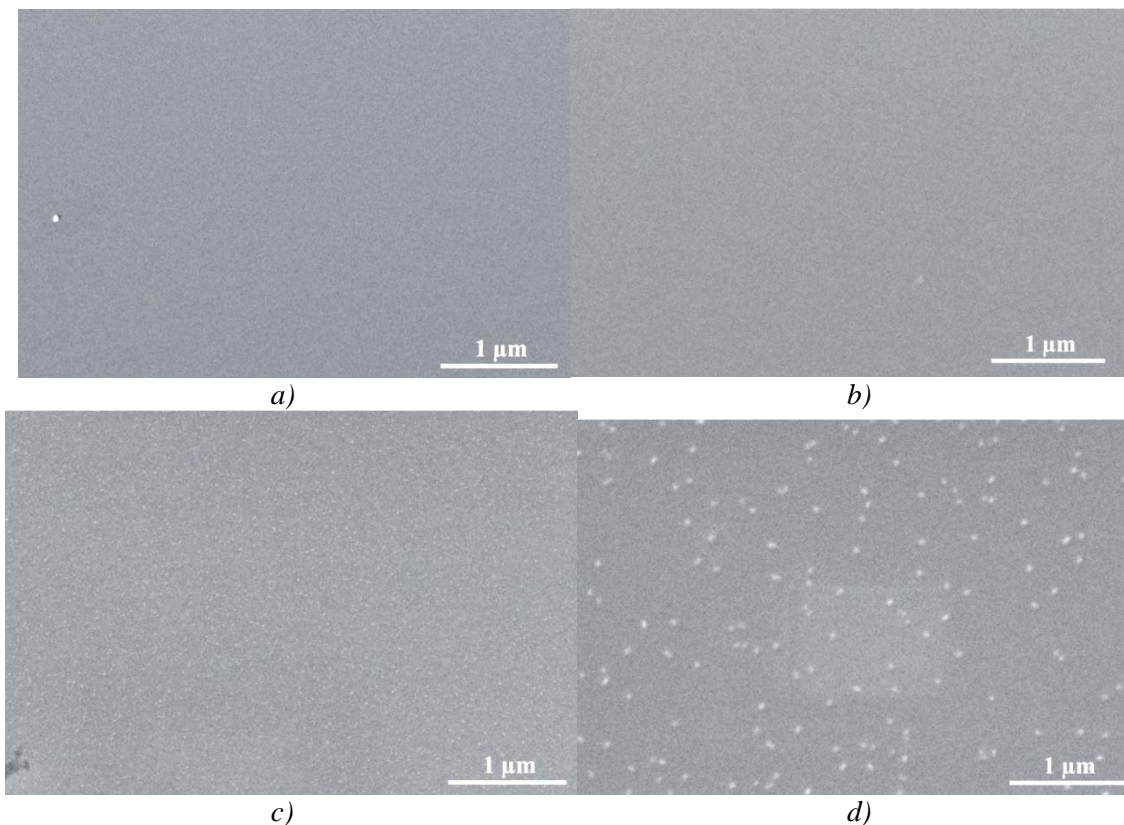

a)   *b)*

c)   *d)*

Fig. 1. Top-view SEM surface morphology for the nanodimensional multilayer structures having a total thickness of 15nm (a), 23nm (b), 43nm (c) and of 203 nm (d), respectively.
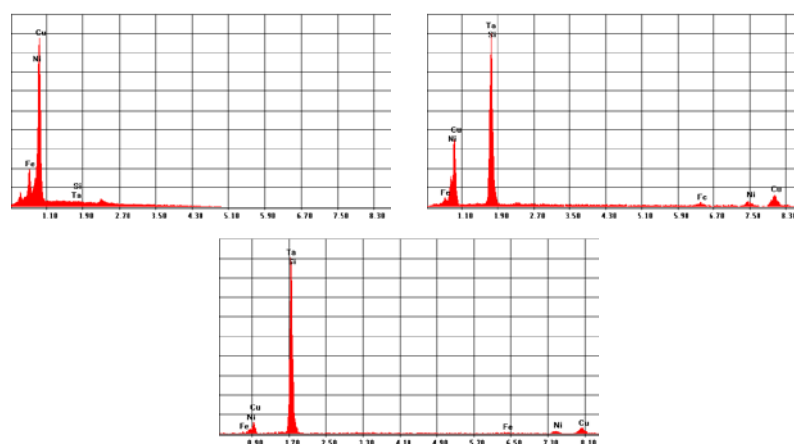

Fig. 2. Examples of X-ray emission spectra obtained by investigating samples having a total thickness of 203 nm, with Si_Cu50Ni50Cu50Fe50Ta3nm structure, at 5 kV (left), 15 kV (centre) and 30 kV (right).

The analysis of the *Ni* layer interfaced with copper layers, showed a drastic decrease in concentration from 7% at 5kV, to 0.2% at 30kV, so the X-rays signal comes from this layer only at very low accelerating voltages, but that do not excite the *K* lines of *Cu*, *Ni* and *Fe*, the results being obtained by *L* lines peak area integration. *Si* concentration, compared with the composition of the layers deposited on it, showed variations between 22% and 30% from 5 to 30kV, which leads to the idea that, regardless of the acceleration voltage, the beam energy significantly penetrate the *Si* layer, hence the majority of the X-ray signal.
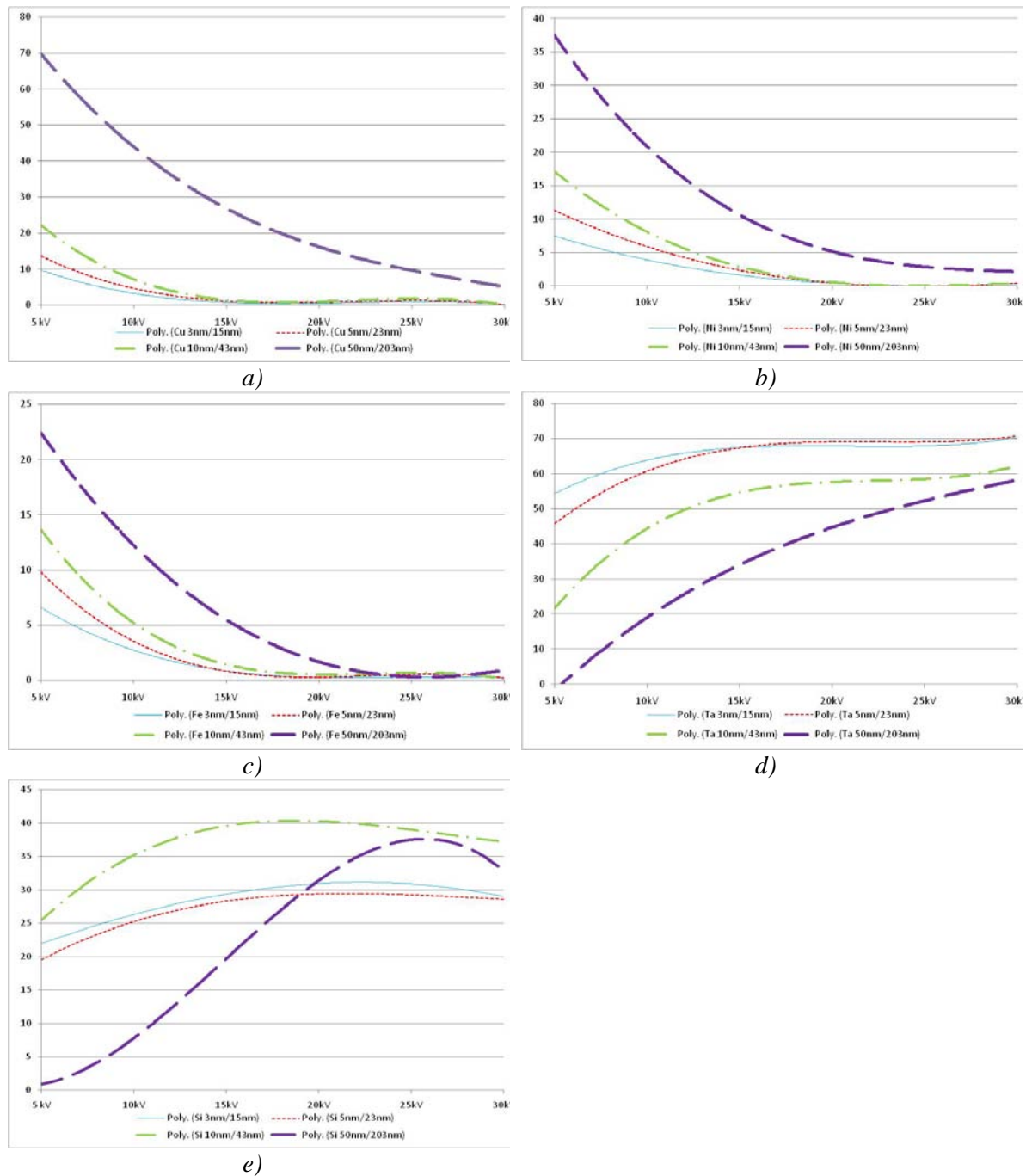
a)

b)

c)

d)

e)

Fig. 3. Varriations of massic concentration of Cu (a), Ni (b), Fe (c), Ta (d) and Si (e), for the layers with tottal thickness 15nm, 23nm, 43nm, respectively 203nm.

Variation of elemental concentrations, of layers of 5nm, with 23nm total thickness, presented similar characteristics with the 3nm layers analysis, the slopes of curves being very close, but concentrations of *Cu*, *Ni* and *Fe* being higher (with about 4%) for tests made at low acceleration voltage. The use of voltages bigger than 20kV revealed concentrations close to the previous layer analysis, so a difference of 2nm for each layer, meaning 8nm totally, is insufficient to significantly influence the interaction volume depth. Variation of *Si* concentration ranks between 20% and 30% from 5kV to 30kV, so the X-ray signal in this case comes mainly from the Si substrate.

Measurements made on 10nm layers heaving the total thickness of 43nm, highlighted concentrations changes, an increase of 2-4% compared with the analysis of 23nm layers at low accelerating voltages, and the trend is similar over 15kV. The significant variation of Si concentration from 24% at 5kV to 42% at higher acceleration voltage indicates that, predominantly at very high energies, the interaction volume includes the characteristic X-ray emission area in the *Si* substrate. At low voltage the energy is sufficient for the excitation of *Cu*, *Ni* and *Fe* nanostructures but being hardly distinguished.

The next analyzed layers had a thickness of 50nm/layer therefore totally 203nm. Compared with the other analyzed structures, in this case the results are very different. At low voltages, the *Si* X-ray signal is almost zero (0.6%) rising to over 30% at high voltage, meaning that *Si* substrate is excited even at this thickness. Using a voltage of 5kV, a *Cu* concentration of 70% was obtained, that decreased by approximately 50% (with 5% for each 5kV), thus in this case the small tensions allowed the excitation of *Cu* layers. A similar trend is present for corresponding signals of *Ni* and *Fe*, the characteristic signal being over 20% at 5kV, meaning that it is sufficiently excited. At voltages lower than 20kV reaches values around 1%, meaning that the beam energy exceeded this layer. The *Ni* concentration is approximately one third of the *Fe* concentration at 5kV, but at 10kV is one third bigger, so this energy is enough to penetrate a multi-barrier of over 100nm. *Ni* concentrations at least double compared to those of *Fe*, were recorded at voltages higher than 20kV.

In order to complete this study, starting from the initial objective of using additional deposited layers made from chemical elements very different from the ones of the structures of interest, we deposited a uniform 500nm layer of silver on each sample. EDS analysis of Cu-Ni-Cu-Fe-Ag samples was made under the same conditions with similar parameters, with the analysis performed on Ag-free layers. Since the thickness of Ag is quite large, in all microanalytical results the Ag concentration was significant.
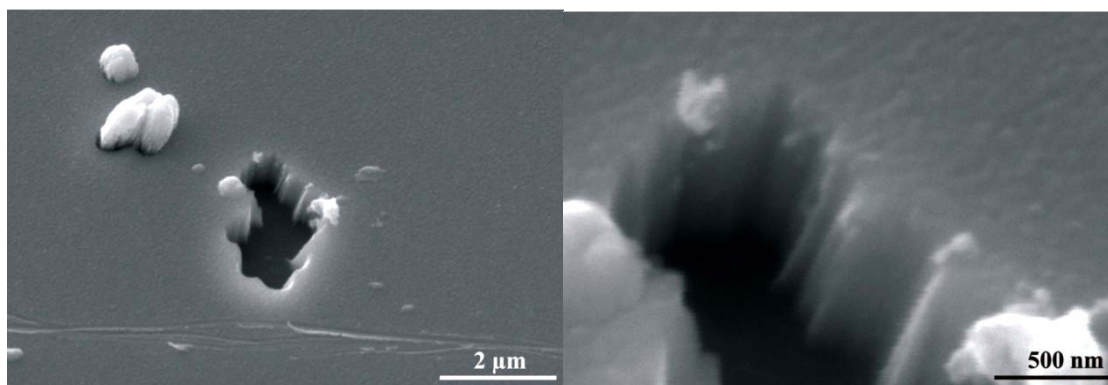

Fig. 4. Top-view SEM surface morphology for the nanodimensional multilayer structures having a 500nm of Ag cover layer.
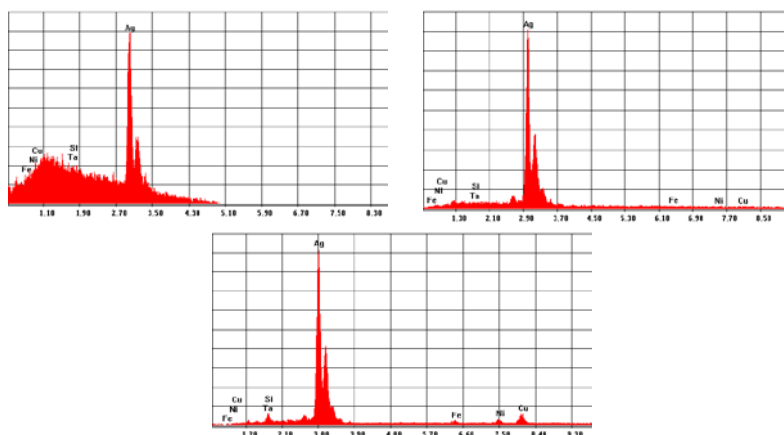

Fig. 5. Representative examples of X-ray emission spectra obtained by investigating samples at 5 kV (left), 15 kV (centre) and 30 kV (right) for Cu50Ni50Cu50Fe50Ta3Ag500 structure.
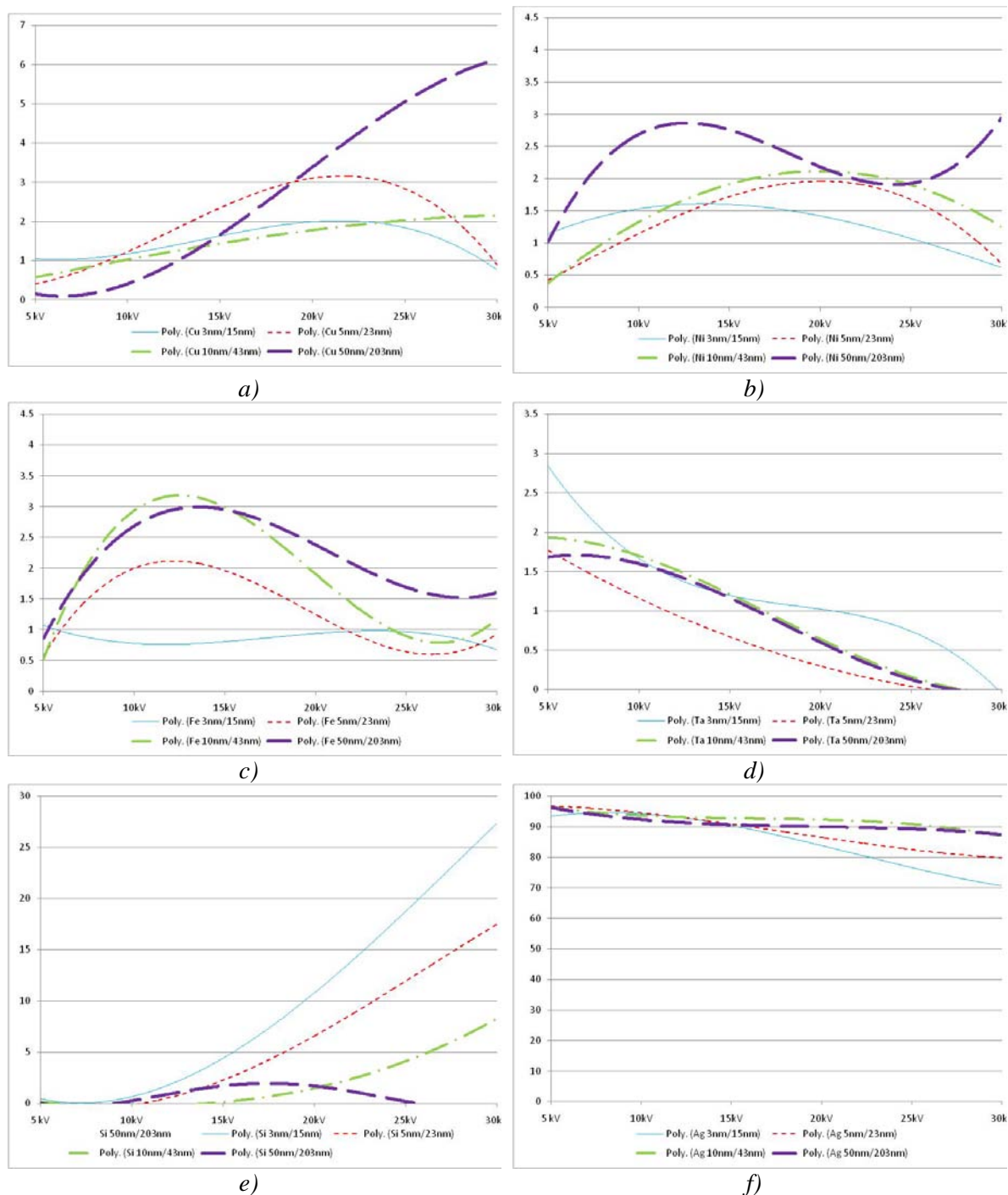
Fig. 6. Varriations of massic concentration of Cu (a), Ni (b), Fe (c), Ta (d), Si (e) and Ag (f) for the layers with total thickness 15nm, 23nm, 43nm, respectively 203nm corresponding to the multilayer structures.

For the first nanostructure, having the thickness of individual layers of 3nm and a total of 515nm, it has been noticed an increased concentration of *Si* from the substrate, from 0.2% at 5kV, to 4% at 15kV, and 27% at 30kV, meaning that the energy at high voltages is big enough to penetrate all layers, and the characteristic X-rays signal to result from the *Si* substrate. On the contrary, the *Ta* layer deposited just under the *Ag* layer, it showed an X-ray signal corresponding to the drop in concentration from 3% at 5kV, to 1.5% at 15kV, and to 0% at 30kV, thus the required energy for atoms excitation was way to high considering the level on which is located the *Ta* layer. Unlike *Ta*, the *Fe* layer gave approximately the same signal in this case, regardless the acceleration voltage of 1%, with a slight decrease at 30kV.

The *Ni* layer (positioned between two layers of copper) signal, ranged between 1% at 5kV, and 1.5% at 10, 15% and 20 kV, followed by a decrease to 0.5% at 25 and 30kV, thus the required energy for atomic excitation of the elements from layers of interest is found between 10 and 20kV, at 10kV, K lines of atoms being unexcited. *Cu* gave a constant signal of approximately 1% for the corresponding energies of 5, 10 and 15kV, a three time increase in concentration at 20kV being observed, followed by a reduction under 1% for 25 and 30kV. In this respect, the appropriate excitation of the *Cu* layer may be at 20kV voltage.

Increasing the thickness of individual layers with 2nm led to *Si* substrate concentration decrease with about 10% for high accelerating voltages, being null at 5 and 10kV voltages. The signal from the thin layer of *Ta* was approximately 2% at 5 and 10kV, gradually decreasing to zero over 15kV, meaning that small accelerating voltages are enough to *Ta* lower lines excitations at depths of 500nm. After a value of 5% at 5kV, *Fe* showed a 2% concentration at 10 kV, gradually decreasing to 1% at 30kV. Similarly to the *Ta* concentration, *Fe* showed the maximum value at 10kV, being possible that this energy is sufficient to excite atoms in this layer, but only from the *L* lines. Unlike *Ta* and *Fe*, *Ni* presented the maximum concentration of 5% at 20kV, increasing by 0.5% from 5 to 15kV and decreasing in the same way over 20kV, being obvious the excitement *Cu* occupied level at the 20kV.

By doubling the thickness of layers, a significant reduction of *Si* concentration was obtained, from 0% at 5 and 10 kV to a maximum of 8% at 30kV. This represents halving the concentrations, compared with the previously analyzed structures. However, the same trend, from 0.2% at 5kV, presents also the *Cu* layer, reaching a constant value of 2% at 25 and 30kV. Thus, at these tensions, we stand close to the energy necessary for 540nm level elements excitation.

Analysis of *Fe* concentrations showed maximum concentration levels at 10 and 15kV of 3%, increasing from 0.5% at 5kV, and then followed by a decrease to 1% at 20, 25 and 30kV. This can lead to the conclusion that this layer is sufficiently excited between 10 and 15kV voltage range, allowing the excitement of the K line. *Ni* showed the maximum concentration of 3% at 20kV accelerating voltage, after a 0.5% increase for each 5kV, and at 25 and 30kV showing concentrations of approximately 1.5%. In this structure case, a direct correlation between the depth at which the X-rays signal was detected and the acceleration voltage electron beam was noticed.

By increasing the individual layer thickness up to 50nm, reaching a total thickness of 703nm, an increase of Si concentration over 20kV with 0.5% for each 5kV was observed. Bellow this threshold the concentration is zero, meaning that the electron beam energy was not sufficient to penetrate the nanostructures. *Ta* concentration was maximum (1.7%) at 5kV and decreased gradually until zero over 25kV. Layers of Cu showed maximum concentrations at 30kV, increasing by 1% for every 5kV, thus the maximum beam energy was sufficient to excite elements from all layers. *Ni* layer, deposited between two layers of *Cu* gave a maximum signal at 25kV, of approximately 2.5% and *Fe* layer of 4% at 15kV. Similarly to the previously analyzed structure, thicker layers confirmed the X-ray signal intensity increasing with the increase of deposited layer depth and with the energy of the electron beam intensity increasing.

4. Conclusions

The performed analysis on layers having individual thickness of 3nm and 5nm, with a total of 15nm and 23nm, pointed out that at any used accelerating voltage, the achievement of the assumption that a double *Cu* concentration compared with the cumulated concentration of *Ni* and *Fe* would be obtained, was not possible. Moreover, quantitative measurements have revealed that at accelerating voltages over 25kV the cumulative concentration of *Ni* and *Fe* is approximately equal to that of *Cu*. In this respect, we propose a different approach meaning the use of low accelerating voltages, but big enough to excite at least the *K* lines of the examined elements. In the analysis of individual layers case, having thicknesses of 10nm and a total of 43nm, the overall trend was similar, but the relation *Cu=Ni+Fe* (in wt% concentration) was valid with great precision at voltages between 15 and 30kV. In this case, the use of 5 and 10kV voltages allows the structure lower layers analysis, but are enough only for *K* lines of elements excitation. In the last structure case (with individual thicknesses of 50nm and 203nm totally) a proportionality of initially assumed concentrations relationship was identified only at 15 and 25kV voltage, but the

outcomes from this relationship at 20 and 30kV. The 10kV difference between the two expected results requires a different approach, especially due to large differences in the data proportionality. Using the maximum acceleration voltage revealed a massive increase in the concentration of *Si*, thus the metallic layer built barrier depth was significantly exceeded.

In the case of silver (500nm) coated layers, especially at high accelerating voltages, the fact that the concentrations relationship *Cu=Ni+Fe* is followed in most cases was observed, except the thinnest layers, of 3nm, for which an intermediate relationship (1.5*Cu=Ni+Fe*) was established. Beginning with the 5nm layers thickness, the proportionality relationship was initially found at 30kV, for the 10nm layers at 25 and 30kV, and for the thick layers from 20kV.

By using additional coating layer of 500nm of silver, has become possible to analyze the nanodimensional multilayer at electron beam acceleration energy of 25 and 30kV, enabling the excitation of *K* lines of heavy elements and determination of a proper proportion between the deposited elements. A disadvantage may occur. It is related with the possibility of greater errors appearance due to the elimination from the integral calculus of the silver corresponding peaks surface, whereas in this case the background correction signal is less precise, and the elements of interest peak-area is smaller.

This data analysis can conclude to the fact that depending on the analyzed chemical elements and their layers thickness, additional coatings can be used (having thickness of a few hundreds of nanometers), of various chemical elements, to study quite precisely the proportion of chemical elements deposited as nanolayers and the depth to which they are located.

Acknowledgements

References

[1] Y. Leng, Materials Characterization - Introduction to Microscopic and Spectroscopic Methods, Hong Kong University of Science and Technology (2008).

[2] D. Brandon, W.D. Kaplan, Microstructural Characterization of Materials, John Wiley & Sons (1999).

[3] J.I. Goldstein, D.E. Newbury, D.C. Joy, C. Lyman, P. Echlin, E. Lifshin, L. Sawyer, J. Michael, Scanning Electron Microscopy and X-ray Microanalysis, 3rd ed., Kluwer-Plenum (2002).

[4] E. Lifshin, X-ray Characterization of Materials, Wiley-VCH Verlag GmbH (1999).

[5] F. L. Ng, J. Wei, F. K. Lai, K. L. Goh, App. Surf. Sci. **252**, 3972 (2006).

[6] V. Juengel, H.J. Ullrich, K.H.Kleinstueck, Wissenschaftliche Zeitschrift, Journal of Alloys and Comp. **23**, 1041 (1974).

[7] P.J. Goodhew, F.J. Humphreys, Electron Microscopy and Analysis, 2nd ed., Taylor&Francis Ltd, London (1988).

[8] J.L. Pouchou, Mikrochim. Acta. **138**. 133 (2002).

[9] I. Jepu, C. Porosnicu, I. Mustata, C.P. Lungu, V. Kuncser, F. Miculescu, Romanian Reports in Physics **62**, 771 (2010).

[10] J. A. Nielsen, C. R. Phys. **9**, 479 (2008).

[11] V. Kuncser, G.Schinteie, P.Palade, I. Jepu, I Mustata, C.P.Lungu, F.Miculescu, G.Filoti, Journal of Alloys and Compounds **499**, 23 (2010).

[12] F. Miculescu, I. Jepu, C. Porosnicu, C.P. Lungu, M. Miculescu, B. Burhala, Digest J. of Nanom. and Biostructures **6**, 307 (2010).

[13] Z. Rouabah, N. Bouarissa, C. Champio, Appl. Surf. Sci. **256**, 3448 (2010).

[14] F.D. Balacianu, A.C. Nechifor, R Bartos, S.I. Voicu, G. Nechifor, Optoelectronics and Advanced Materials-Rapid Communications **3**, 219 (2009).